Research Square

Preprints are preliminary reports that have not undergone peer review.
They should not be considered conclusive, used to inform clinical practice,
or referenced by the media as validated information.

Host-guest Encapsulation of Photosensitizer to Construct Antibacterial Silicone Rubber: Enhanced Homogeneity and Dual-action

Jin Han
Zhejiang University of Technology
Yaocheng Zhu
Zhejiang University of Technology
Ziqiang Zhang
Zhejiang University of Technology
Taolei Qiu
Zhejiang University of Technology
Lei Wang
Zhejiang University of Technology
Zhengping Zhao
Zhejiang University of Technology
Xiaoxue Yin
Zhejiang Tongxuan Medical Technology Co., Ltd
Dawei Zhang
Zhejiang Tongxuan Medical Technology Co., Ltd
Kun Shen
txshenkun@163.com

Zhejiang Tongxuan Medical Technology Co., Ltd
Dong Xu
Polymer Research Institute, Wenzhou Gettel High-Tech Materials Co., Ltd
Boshi Yu
Polymer Research Institute, Wenzhou Gettel High-Tech Materials Co., Ltd
Tongdong Shen
Interdisciplinary Research Academy
Zhixiong Liu
Shanxi Datong University

Research Article

Keywords: Silicone Rubber, Photodynamic, Amphiphilic HQAS, Antibacterial

Posted Date: August 25th, 2026

DOI: https://doi.org/10.21203/rs.3.rs-10578588/v1

License: This work is licensed under a Creative Commons Attribution 4.0 International License.
Read Full License

Additional Declarations: No competing interests reported.

Host-guest Encapsulation of Photosensitizer to Construct Antibacterial Silicone Rubber: Enhanced Homogeneity and Dual-action.

Jin Han[1], Yaocheng Zhu[1], Ziqiang Zhang[1], Taolei Qiu[1], Lei Wang[1], Zhengping Zhao[1], Xiaoxue Yin[2], Dawei Zhang[2], Kun Shen[2,*], Dong Xu[3], Boshi Yu[3], Tongdong Shen[4], Zhixiong Liu[5]

1) State Key Laboratory of Advanced Separation Membrane Materials, Zhejiang Key Laboratory of Advanced Polymer Materials Modification and Application Technology, Zhejiang University of Technology, Hangzhou, 310014, PR China

2) Zhejiang Tongxuan Medical Technology Co., Ltd., Hangzhou, 317300, PR China

3) Polymer Research Institute, Wenzhou Gettel High-Tech Materials Co., Ltd, Wenzhou, 325802, PR China

4) Zhejiang Collaborative Innovation Center for Full-Process Monitoring and Green Governance of Emerging Contaminants, Interdisciplinary Research Academy, Hangzhou 310015, China

5) College of Chemistry and Chemical Engineering, Shanxi Datong University, Datong, 037009, PR China

Correspondence to: txshenkun@163.com

ABSTRACT

An efficient process for the construction of antibacterial silicone rubber by a combined action of multiple quaternary ammonium salts (QAS) functionalities and photodynamic process through host-guest encapsulation of photosensitizer Rose Bengal (RB) into amphiphilic hyperbranched quaternary ammonium salts (Am-HQAS) nanocapsules was developed. RB is incompatible with silicone rubber, but the host-guest complexation between RB and Am-HQAS could make RB homogenously dispersed in silicone rubber matrix and wash-resistant. When the amphiphilic HQAS was incorporated into silicone rubber through tertiary amino group-initiated epoxy ring-opening reaction, the modified silicone rubber samples, RTV-Am_x series, could reach an antibacterial efficacy of 94% and 96% for *Escherichia coli* (*E. coli*) and *Staphylococcus aureus* (*S. aureus*), respectively. Efficacy was found to increase with increasing quaternization degree of the embedded Am-HQAS. After encapsulating RB, the resulted e-RTV-Am_{60}-RB sample could release singlet oxygen $^1O_2$ under LED light irradiation and the killing rate after light irradiation increased to 98% and 99% for *E. coli* and *S. aureus*, respectively. The e-RTV-Am_{60} sample exhibited a yield strength of 0.73 MPa and a compressive modulus of 25 MPa, much larger than that of raw silicone rubber. A negligible change of comprehensive strength after multiple loading-unloading cycles suggested excellent elasticity and shape recovery ability. The excellent mechanical strength and high antibacterial efficacy could render the presented materials interesting for healthy and medical applications. Besides, it is believed that other hydrophilic photosensitizers are also applicable to this host-guest system.

Keywords: Silicone Rubber; Photodynamic; Amphiphilic HQAS; Antibacterial

INTRODUCTION

Silicone rubber is one of the most widely used and valuable class of polymer materials in various industries like aerospace, electronics, medical and food processing industry [1-3]. The skeleton of silicone rubber is mainly composed of silicone and oxygen atoms and thus exhibits unique properties including outstanding mechanical strength, chemical stability, biological inertness and good biocompatibility. For example, silicone rubber catheters are widely used in medical and clinic areas including long-term implants and short-term indwelling devices in the body [4-6]. However, the hydrophobic surface of the silicone rubber would cause serious bacterial proliferation and adhesion when implanted in a physiological environment, which resulted in adverse effects in the function and durability of the materials [7-8]. These adverse effects would induce wound infection, inflammation, thrombosis and high morbidity. Antimicrobial behavior under physiological conditions is a desirable attribute for silicone rubber used in implants as the antimicrobial behavior can alleviate the attachment of bacteria and inhibit the formation of biofilms. A facile and efficient method to render silicone rubber antibacterial property is to introduce antibacterial agents. However, traditional antibiotic-coated or impregnated silicone rubber are only suitable for short-term applications [9-10].

QAS derivatives are found to be an efficient antibacterial agent to fabricate antibacterial silicone rubber due to the broad-spectrum antimicrobial activity against bacteria, long-term durability and environmentally friendliness [11-14]. Tang et al developed an intrinsic antibacterial silicone rubber with matrix tethering quaternary ammonium salt groups and the silicone rubber exhibited effective antibacterial activity and antibacterial durability even with low QAS group content [12]. As a kind of QAS, quaternized hybranched polyethylenimine

(HPEI) nanoparticles with multiple QAS groups were introduced into polyurea resin [15] and hydrogel [16-19] to fabricate antibacterial materials and the hyperbranched QAS nanoparticles showed high contact-killing efficacies. Amphiphilic hyperbranched QAS nanocapsules consisting of a hydrophilic hyperbranched QAS "head" and multiple hydrophobic long carbon chain could provide effective bacterial contact-killing performance because the hydrophobic alkyl could facilitate the quarternary ammonium salt penetrating the cell membrane to kill the bacteria [20-21]. However, there are few works introducing hyperbranched QAS nanocapsules to develop antibacterial silicone materials.

Photodynamic antibacterial chemotherapy (PACT) is an effective and low-cost antibacterial strategy [22-26]. The excitation of a photosensitizer with appropriate light could generates reactive oxygen species (ROS), which is responsible for the attack on organic structures and thus for the killing of germs [27]. PACT technology could be repeatedly used but showed negative antibiotic resistance. Also, it has efficient phototoxic activity against antibiotic-resistant microbial strain. Therefore, the PACT technology has evolved to compete with or replace antibiotics, reducing the burden of antibiotic resistance [28-30]. More importantly, the high reactivity of ROS makes the bacteria being killed in a very short time, suggesting a high antibacterial efficiency [31-32]. Therefore, PACT could effectively solve the problem of slow sterilization of silicone rubber containing antibacterial agents. Fortunately, amphiphilic hyperbranched QAS could be also used as nanocapsules to encapsulate the soluble photosensitizer as the guest molecules owing to the abundant of intramolecular cavities through host-guest encapsulation [33-34]. The amphiphilic hyperbranched QAS loaded with photosensitizer could be well-dispersed into silicone rubber to provide durable bactericidal

effect. A combination of hyperbranched QAS with contact-killing and PACT is expected to enhance the antibacterial effect of silicone rubber. To the best of our knowledge, there is no report of antibacterial silicone rubber preparing through combing a contact-killing strategy with PACT. In this paper, Am-HQAS was used as a host to encapsulate the photosensitizer RB through host-guest encapsulation and was introduced into silicone rubber to develop antimicrobial silicon rubber. The multiple QAS would provide an efficient bacterial contact-killing performance. PACT could effectively solve the problem of slow sterilization of QAS functionalities. Therefore contact-killing and PACT could effectively enhance the antibacterial activity of the silicone rubber.

EXPERIMENTAL SECTION

Materials. PDMS-OH for silicone rubber was purchased from Shandong Bogang Biotechnology Co., Ltd. Tetraethoxysilane (TEOS) and 3-glycidyloxypropyltrimethoxysilane (KH560) were obtained from Shanghai Titan Scientific Co., Ltd. Dibutyltin dilaurate (DBTDL) was acquired from Shanghai Aladdin Bio-Chem Technology Co., Ltd. Hydrophobic fumed silica (SiO_2), R812S, was obtained from Evonik Degussa. HPEI (Mn~10000 by GPC) was purchased from Sigma-Aldrich. Chloroacetic acid and cetyl alcohol were obtained from Shanghai Macklin Biochemical Co., Ltd. Formic acid, formaldehyde and *p*-toluene sulfonic acid were acquired from National Pharmaceutical Group Chemical Reagent Co., Ltd. The other reagents were used as received.

*Synthesis of Am-HQ*AS

Methylated hyperbranched polyethyleneimine (MeHPEI) and cetyl chloroacetate (CCA) were

synthesized according to the reported literature [33, 35]. Am-HQAS were prepared as follows: To a 100 mL round bottom flask, MeHPEI (1.0 g), certain weights of CCA and dried toluene (5 mL) were added. The mixture was continued to stir at 60 ℃ for 48 h. Then, 100 mL of ethyl acetate was added and the mixture continued to stir for 20 min. The mixture was centrifuged and the precipitate was dried in vacuum. These Am-HQAS nanocapsules are referred to Am_x-HQAS, where x represents the quaternization degree. The quaternization degree was calculated by the weight ratio of MeHPEI/CCA according to the reported literature [33]. The feed ratios of the various samples were presented in Table S1.

Preparation of the host-guest complex between Am_{60}-HQAS and RB, RB@Am_{60}-HQAS

100 mL of RB aqueous solution (2.054 mg/mL) was added into 100 mL of Am_{60}-HQAS in chloroform (0.01 mg/mL). The mixture continued to stir for 30 min. The organic phase was separated and dried with anhydrous $MgSO_4$. After filtration, the solvents were removed under reduced pressure to provide RB@Am_{60}-HQAS as a red solid.

Determination of the encapsulating capabilities for photosensitizer RB

RB was placed into 500 mL volumetric flask, followed by dissolving with ultrapure water to a concentration of 1.0-10 μg/mL. The absorbance at 540 nm wavelength was recorded by ultraviolet-visible-near infrared absorption spectrum (UV-VIS-NIR) (Lambda 950). The absorbance values at 540 nm obtained with the respective concentration were recorded and plotted. Linear relationships between absorbance values and concentration resulted in a standard work curve and were shown in Fig. S1.

In the adsorption experiment, taking the Am_{60}-HQAS as an example, Am_{60}-HQAS (0.50 g) was placed into 50 mL volumetric flask, followed by dissolving with chloroform to the

concentration of 0.01 g/mL. A series of RB solutions with different concentrations in range of 0.1-3.2 mg/mL was prepared. Typically, equal volumes of a chloroform solution of Am_{60}-HQAS and a certain concentration of RB solution were pipetted into a vial and the vial was continued to stir for 20 min. After phase separation, it was observed that the chloroform phase was dyed red. The upper water phase was analyzed by UV-VIS-NIR spectroscopy to calculate the amount of the remained RB in the aqueous phase according to the corresponding standard curve, and thus the amount of the RB transported to Am_{60}-HQAS could also be calculated. Therefore, the encapsulating capability *vs* the RB concentration was plotted (Fig. S2). According to the encapsulation curve, the amount of RB loaded into Am_{60}-HQAS was 0.2 g/g. Namely, 1.0 g Am_{60}-HQAS could encapsulate 0.2 g RB under this condition.

Preparation of antibacterial silicone rubber using Am-HQAS or RB@Am_{60}-HQAS

PDMS-OH and/or SiO_2 were mixed and stirred vigorously for 20 min. Then Am-HQAS (or RB@Am_{60}-HQAS) in toluene and KH560 were added into the above prepared mixture and heated to 70 ^{o}C under stirring. The mixture continued to stir for 9 hours. Then a certain amount of TEOS was added and then the air bubbles were removed under reduced pressure. DBTDL catalyst was added in and stirred for 3 min under reduced pressure. Finally, the mixture was poured into a pre-designed transparent PTFE mold and cured for 7 days to obtain a series of antibacterial silicone rubber. The antibacterial silicone rubber with Am_x-HQAS was referred to RTV-Am_x, where the x represents the quaternization degree of Am_x-HQAS. The silicone rubber with SiO_2 and TEOS was referred to e-RTV, and the e-RTV with Am_{60}-HQAS and RB@Am_{60}-HQAS was referred to e-RTV-Am_{60} and e-RTV-Am_{60}-RB, respectively. The feed ratios of the various samples were presented in Table S2.

Characterization

Chemical characterization was performed by ^{1}H NMR spectroscopy using a Bruker AVANCE III 500 MHz. Chemical shifts were reported in parts per million (ppm) relative to the internal standards, $CDCl_3$ solvents or tetramethylsilane. The structure of the silicone rubber was characterized by UV-VIS-NIR. The wetting of the coatings was measured by an automatic optical contact angle tester (Dataphysics OCA30).

Compressive test

The tensile and compressive strength of the samples was tested by a high and low temperature tensile-compressive tester (Instron 5996, Instron Co.). The tensile test was carried out according to Chinese Standard GBT528-1998 "Rubber, vulcanized or thermoplastic. Determination of tensile stress-strain properties". Dumbbell shaped type I sample was used for tensile test and the tensile speed was set to 20 mm/min. The samples with a diameter of 15 mm and a height of 4 mm were used to perform compressive tests. The compressive test was repeatedly conducted 10 times at a speed of 1 mm/min, and the maximum compression deformation was 60%. Each sample was measured three times.

Detection of singlet oxygen $^{1}O_2$

RB can produce ROS (e.g. singlet oxygen $^{1}O_2$) under light irradiation. According to the reported literature [36-37], 1,3-diphenylisobenzofuran (DPBF) could be used as the capture agent to capture $^{1}O_2$ and the concentration of $^{1}O_2$ could be measured by determining the concentration of DPBF detected by ultraviolet visible spectrophotometer. In this experiment, 100 mL of DPBF ethanolic solution (0.03 g/L) was prepared. Then the e-RTV-Am_{60}-RB sample was placed into a 12-hole plate and 4.0 mL DPBF ethanolic solution was injected into

the holes. The sample was first kept in the darkness for 5 min and then irradiated with an LED lamb for 0 min, 1min, 3min, 5min, 10min, 20min and 30min. After irradiation, the absorbance value of the DPBF ethanolic solution in the range of 250 to 800 nm was measured by UV-VIS-NIR.

Antibacterial test

E. coli and *S. aureus* were chosen as model bacteria to study the antibacterial property of the prepared silicone rubber. The selected strains were evenly coated in the dish containing solid culture medium, sealed with sealant and kept in a 37 ºC incubator for 12 hours. A single colony of bacteria was used to inoculate Luria-Bertani (LB) liquid culture separately at 37 ºC for 12 hours. Then a certain volume of the suspension was taken out and diluted to a certain concentration (at 600 nm wavelength, OD_S=~0.05, OD_E=~0.1).

(1) Determination of the antibacterial ability

The silicone rubber was cut into 15×15 mm thin slice and immersed into ethanol for 3 days. The dried silicone rubber sample was placed into a twelve-well plate and sterilized by UV light irradiation for 30 minutes. Then 3 mL of diluted LB liquid culture medium was injected into each well and incubated at 37 °C for 24 hours. The e-RTV-Am_{60}-RB sample was irradiated with an LED lamp for 10 min, but the other sample was kept in the darkness. Finally, the samples were washed with PBS buffer to remove the non-adherent bacteria. Bacteria adhering on the surface of the silicone rubber was dyed by dropping diluted Live/Dead BackLight Kit (Thermo Fisher Scientific Inc., NY) and observed with an Axio Observer (Carl Zeiss Jena., OBSERVER) inverted fluorescence microscope under a 40-fold objective lens. Each experiment was carried out in triplicate. The antibacterial ability R is relative to the viable

bacteria and calculated as follows:

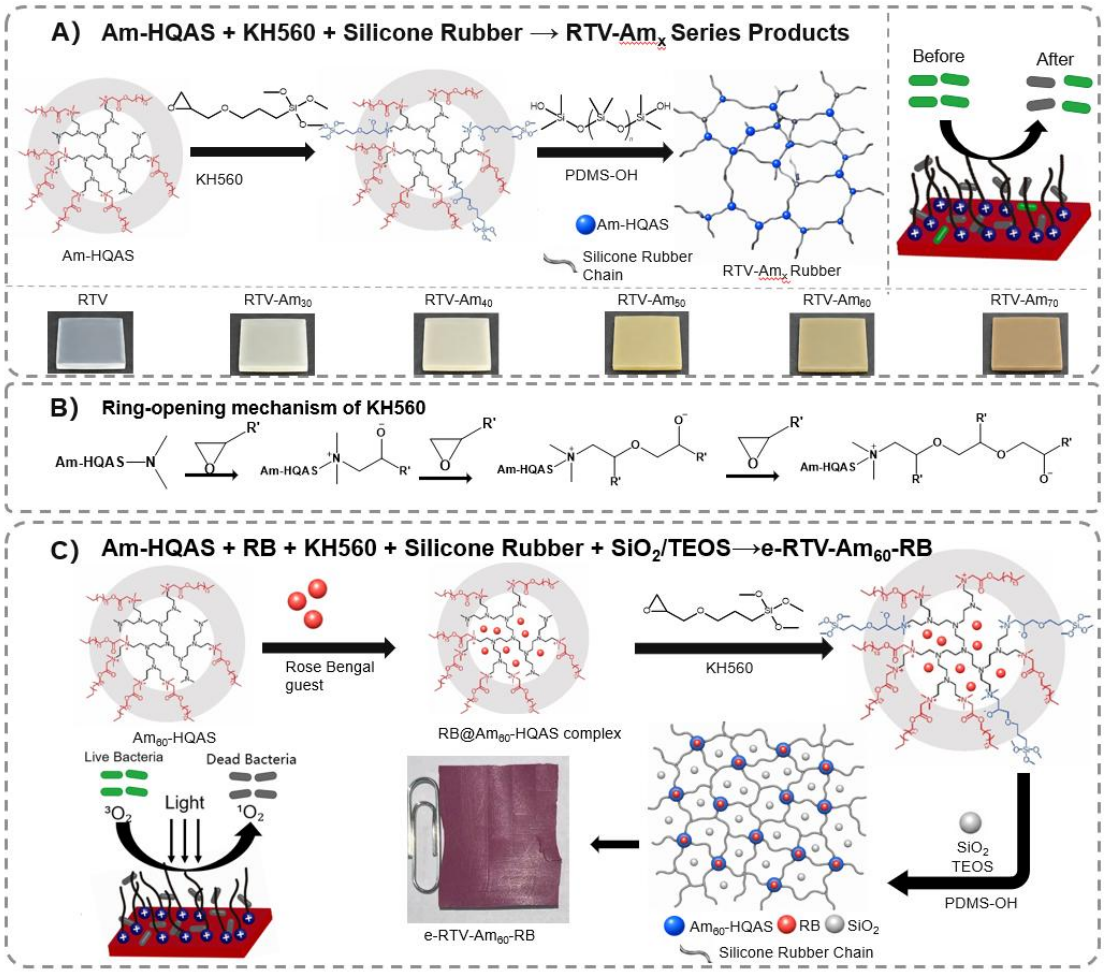
$$R = (N_O - N_R) / N_O \times 100\%$$

Where N_0 is the number of bacterial colonies on the control sample and N_R is the number of bacterial colonies on the antibacterial silicone rubber.

To evaluate the antibacterial performance of the antibacterial silicone rubber for long time, the sample coated with 3 mL of diluted LB liquid culture medium was incubated at 37 °C for a long time (e.g. 12, 24, 36, 48, 72 h). The following detection procedure was similar with above mentioned procedure.

(2) Determination of the bacterial growth curve

The silicone rubber was cut into 10×10 mm thin slice and immersed into ethanol for 3 days. The dried silicone rubber sample was placed into a 1 cm cell and sterilized by UV light irradiation for 30 minutes. Then 2 mL of diluted LB liquid culture medium was injected into the cell with a holder and incubated at 37 °C for 24 hours. The absorbance value at ~600 nm wavelength was measured by UV-VIS-NIR at regular intervals.



Scheme 1. (A) Preparation of RTV-Am$_x$ series silicone rubber samples and their actual pictures; (B) Residual tertiary amino groups-initiated ring-opening mechanisms of epoxy groups in KH560; (C) Synthetic route of RB@Am$_{60}$-HQAS complex and e-RTV-Am$_{60}$-RB silicone rubber sample and the actual picture.

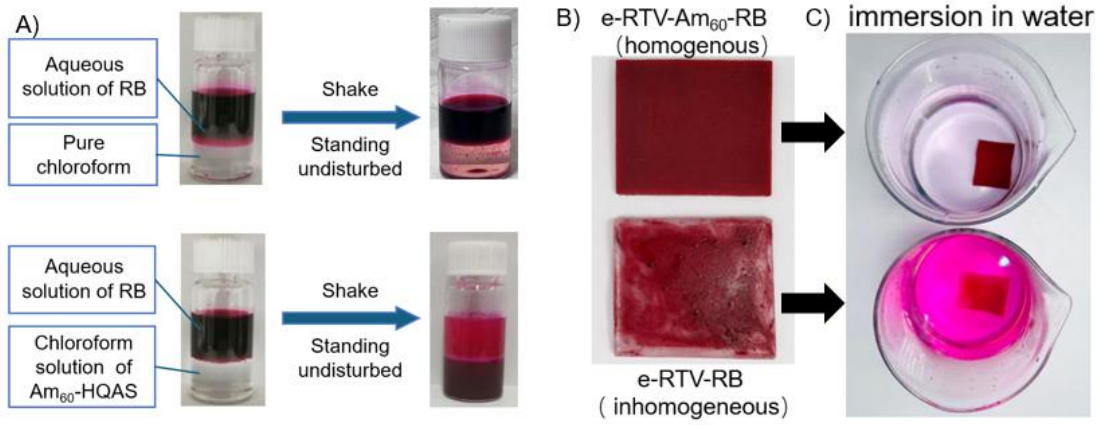


Fig. 1 (A) Host-guest encapsulation process between RB guest and Am60-HQAS host; (B) The

actual pictures of the homogenous e-RTV-Am60-RB sample and the inhomogeneous e-RTV-RB control sample without using Am60-HQAS host; (C) The water immersion test for e-RTV-Am60-RB sample and the control one.

RESULTS AND DISCUSSION

The preparation route of the RTV-Am_x series samples and the e-RTV-Am_{60}-RB sample were presented in Scheme 1A and 1C, respectively. Quaternarization of MeHPEI with CCA resulted in Am-HQAS nanocapsules with multiple hydrophilic QAS moieties in the core and many long carbon chains through betaine ester-linked bonds as the hydrophobic shell (Scheme S1). The residual tertiary amine groups triggered a ring-opening reaction with the epoxy groups in KH560 (Scheme 1B), and the introduced trimethoxysilyl group chemically bonded Am-HQAS into silicone rubber to give RTV-Am_x samples (Scheme 1A). In Scheme 1C and Fig. 1A, a facile phase transfer method was used to form a host-guest RB@Am_{60}-HQAS complex between RB and Am_{60}-HQAS. By utilizing the Am_{60}-HQAS host, a significant amount of deep red RB can be transferred from the aqueous phase to the chloroform phase, thereby imparting a deep red color to the chloroform phase. The RB@Am_{60}-HQAS complex was then chemically bonded into silicone rubber by means of KH560 coupling agent to obtain e-RTV-Am_{60}-RB. In this way, RB was homogenously dispersed in silicone rubber matrix and wash-resistant, and e-RTV-Am_{60}-RB possesses dual antibacterial actions: contact antibacterial activity of QAS and PACT antibacterial activity of RB. In contrast as shown in Fig. 1B and 1C, the e-RTV-RB sample prepared without the aid of Am_{60}-HQAS exhibited an inhomogeneous state, and the RB within the sample readily diffused into water during the water immersion test.

The number of QAS functionalities determining the antibacterial ability was related to the degree of quaternization. The quaternization degree of Am-HQAS was calculated according to ^{1}H-NMR spectrum [33] (Fig. S3). The degree of quaternization of Am_{30}-HQAS, Am_{40}-HQAS, Am_{50}-HQAS, Am_{60}-HQAS and Am_{70}-HQAS was 30.0%, 39.2%, 49.1%, 58.5 and 65.1%, respectively, similar with the feed ratio of CCA/MeHPEI. The quaternization reaction is highly active. With increasing of the feed ratio of CCA/MeHPEI, the degree of quaternization showed an increasing trend. Therefore, the degree of quaternization could be finely tuned by adjusting the feed ratio of CCA/MeHPEI.

The chemical structure of Am-HQAS and antibacterial silicone rubber were further characterized by FT-IR. From Fig. 2A, the adsorption peak at 2915 and 2850 cm^{-1} were assigned to the stretching vibration peaks of -CH_2- group. The peak centered at 1467 cm^{-1} was attributed to the bending vibration of methene groups. After coupled with CCA, peaks at 1740 and 1202 cm^{-1} were ascribed to the stretching vibration of the carbonyl (C=O) group and the C-O-C stretching vibration in the ester bond, respectively. The characteristic absorption peak at 908 cm^{-1} assigned to the stretching vibration of the -C-N^+- group and no appearance of C-Cl bond near 800 cm^{-1} (indicating the cleavage of the C-Cl bond) confirmed a successful quaternization process. As shown in Fig. 2B, the silicone rubber containing Am-HQAS showed a similar adsorption spectrum with RTV after the Am-HQAS being blended with silicone rubber. The strong adsorption peaks at 2915 and 2850 cm^{-1} were assigned to the stretching vibration of -CH- group. The peaks at 1257 and 790 cm^{-1} were attributed to symmetrical stretching vibration and deformation vibration of -CH_3 group. The adsorption bands at 1075 and 1007 cm^{-1} were according to stretching vibration of Si-O-Si. The weak adsorption bands

at 2850 and 1740 cm^{-1} were assigned to the stretching vibration peaks of N-CH_2- and C=O groups, suggesting Am-HQAS was successfully introduced into silicone rubber.

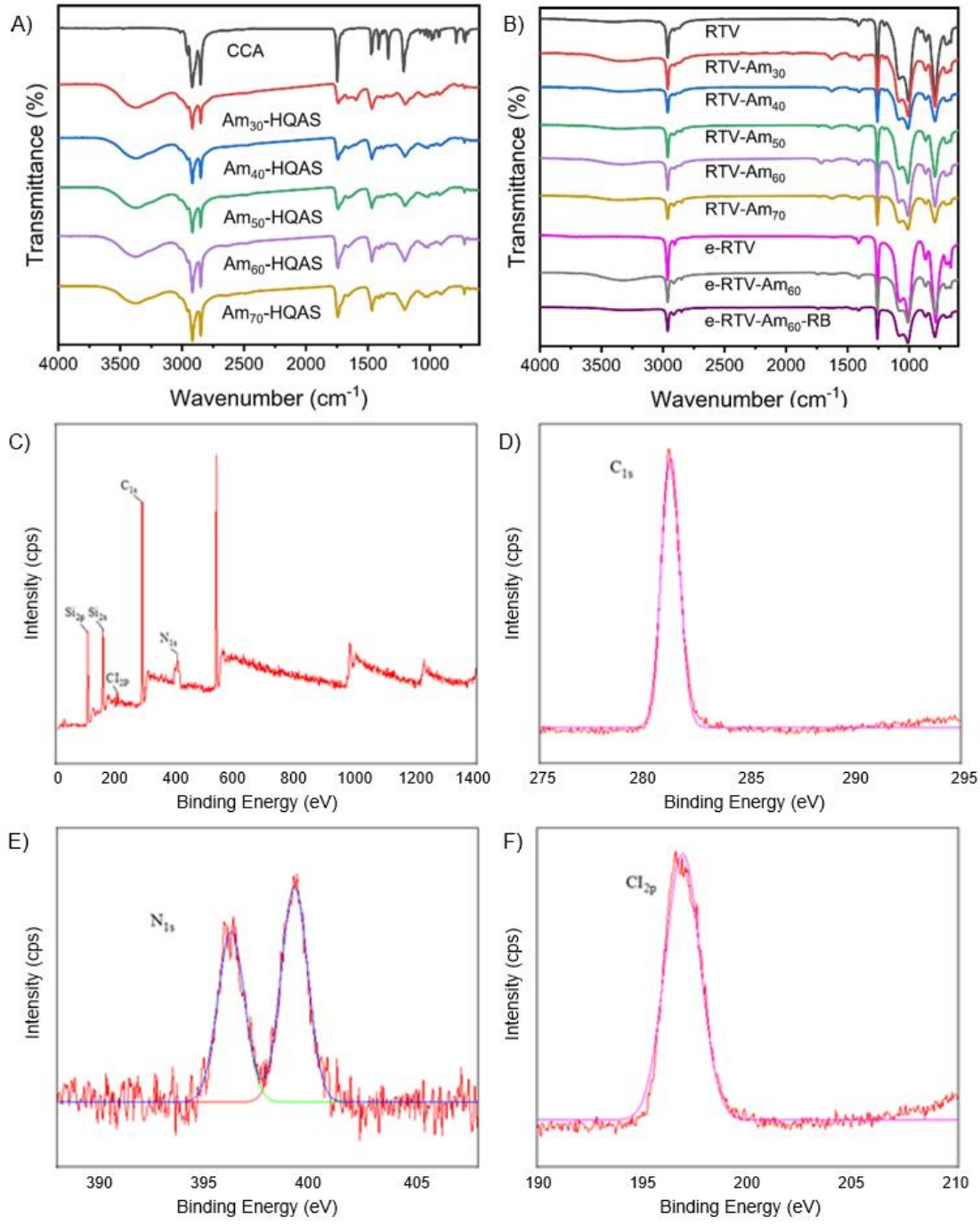


Fig. 2 FT-IR spectra of Am-HQAS (A) and the resulted silicone rubber samples (B); XPS spectra of e-RTV-Am60-RB (C, D, E, and F).

To further confirm the structure of the e-RTV-Am_{60}-RB sample, XPS analysis was performed.

In Fig. 3, the bands at 196 and 399 eV were ascribed to Cl2p and N1s transitions, respectively. The N1s band can be deconvoluted into two peaks with binding energies at 396.2 and 399.3 Ev (Fig. 2E), which correspond to the quaternary ammonium salt group formed from KH560 and CCA, respectively. The results confirmed the Am-HQAS was successfully dispersed into the siloxane rubber network.

Wettability of silicone rubber

The static water contact angle (CA) on the surfaces of the prepared silicone rubber was measured. The CA of the RTV was 114.6°. However, after adding Am-HQAS into the silicone rubber, the value of CA increased with the increasing of quaternizations degree. The CAs of RTV-Am_{30}, RTV-Am_{40}, RTV-Am_{50}, RTV-Am_{60} and RTV-Am_{70} were 116.9°, 119.7°, 125.1°, 128.0° and 128.9°, respectively (Fig. S4). The increased quaternization degree caused a large abundance of hydrophobic fatty chains enriched on the outer surface of the silicone rubber and finally resulted in a more hydrophobic surface. After encapsulating photosensitizer RB, the CA of e-RTV-Am_{60}-RB decreased to 103.3°, smaller than the value of e-RTV-Am_{60} (Fig. S5). This change was attributed to the more hydrophilic RB guest.

Mechanical properties

The mechanical properties of antibacterial silicone rubber were investigated by tensile compression. From Fig. S6 and Fig. 3A, the tensile strength and elongation at break of the RTV was 0.54 MPa and 75%, respectively. When modified with Am-HQAS, the tensile strength at break of antibacterial silicone rubber decreased but their elongations at break increased. With increasing of quaternization degree, the tensile strength showed a first increase then decrease trend. The tensile strength at break of RTV-Am_{30}, RTV-Am_{40}, RTV-Am_{50}, RTV-Am_{60} and RTV-

Am_{70} was 0.30, 0.41, 0.48, 0.34 and 0.35 MPa, respectively (Fig. 3A). The elongation at break showed a decrease trend with increased quaternization degree. The elongation at break of RTV-Am_{30} was the largest, up to 230% (Fig. 3A).

The compressive strength of the samples was further tested. From Fig. S7, at compressive strains below 10% the response of the sample was predominantly elastic (as confirmed by the linear stress-strain relation). With increasing compressive strains from 10% to 50%, the compressive stress increased slowly and exhibited nonlinear behavior. Once compressive strain was larger than 50%, the compressive stress showed a sharp increase. During the unloading process, strain hysteresis was observed and attributed to a time-delayed elastic response since all the silicone rubber eventually displayed complete shape recovery. The results of compression testing were summarized in Fig. 3B. The compressive stress and elastic modulus of RTV were 2.9 and 16 MPa, respectively. Compared with that of RTV, the compressive stress and elastic modulus of RTV-Am_x decreased, probably due to the decrease of the crosslinking density. With the increase of Am-HQAS, the maximum compressive stress showed a first increase and then decrease trend. For example, the maximum compressive stress of RTV-Am_{30}, RTV-Am_{40}, RTV-Am_{50}, RTV-Am_{60} and RTV-Am_{70} was 1.9, 2.0, 2.3, 2.7 and 2.2 MPa, respectively. The elastic modulus showed a similar trend. The mechanical strength of the samples after multiple loading-unloading cycles has been examined to evaluate the stability and durability of the samples. As for raw RTV sample, the comprehensive load showed a significant decrease with increasing the loading-unloading cycles (Fig. S8A). In contrast, the maximum load of the RTV-Am_x samples showed a negligible decrease with increasing the loading-unloading cycles (Fig. S8B-F). The stability and durability of the RTV-Am_x samples

were attributed to the flexibility of the hyperbranched structure of Am-HQAS. [19, 33]

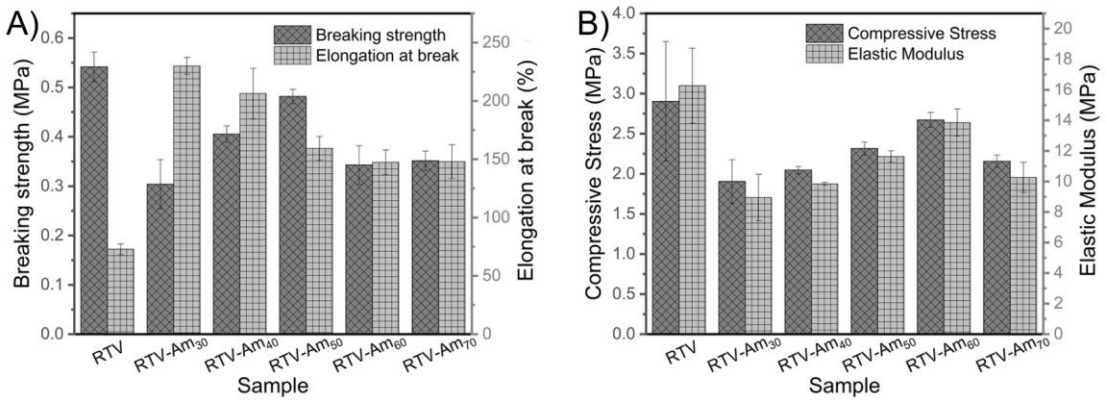


Fig. 3 Breaking strength and elongation at break (A) and compressive stress and elastic modulus (B) of the RTV and RTV-Amx samples.

Although the RTV-Am_x samples showed excellent stability and durability, the tensile strength and comprehensive stress was poorer than the raw RTV. To overcome this limitation, TEOS with four active sites was used as a co-curing agent to increase the crosslinking density. Moreover, SiO_2 was introduced into the silicone rubber to further improve their mechanical strength. The feed ratio was presented in Table S2. From Fig. 4A, compared with that of e-RTV, the tensile strength and elongation at break of e-RTV-Am_{60} and e-RTV-Am_{60}-RB showed a sharp increase. The tensile strength at break of e-RTV-Am_{60} and e-RTV-Am_{60}-RB was 0.73 and 0.80 MPa, respectively (Fig. 4B), increased ~67%. The elongation at break of e-RTV-Am_{60} and e-RTV-Am_{60}-RB was 212 and 228% (Fig. 4B), respectively, increased ~65%. A reasonable explanation was that the introducing co-curing agent facilitated forming a dense silicone rubber matrix and the hyperbranched structure of Am-HQAS further increased the compatibility of SiO_2 in silicone rubber, resulting in an improved strength and toughness of the system. The compressive strength of the silicone rubber was also tested. The comprehensive stress-strain curve of the above sample was similar with the RTV-Am_x samples (Fig. 4C). The compressive

stress and elastic modulus of e-RTV-Am_{60} were 5.2 and 25 MPa (Fig. 4D), respectively, much larger than that of RTV-Am_{60} and e-RTV. After blending with Am-HQAS, the value of the compressive stress and elastic modulus decreased but was a little larger than that of e-RTV. Fig. S9 showed the comprehensive strength of the samples after multiple loading-unloading cycles. The maximum load of the samples showed a negligible decrease with increasing the loading-unloading cycles. The above results showed that the silicone rubber matrix has not been obviously affected after multiple repeated loading and unloading process, indicating excellent elasticity and shape recovery ability. In all, the mechanical strength of the antibacterial silicone rubber was effectively improved due to a combined action of SiO_2 and the hyperbranched Am-HQAS. [38]

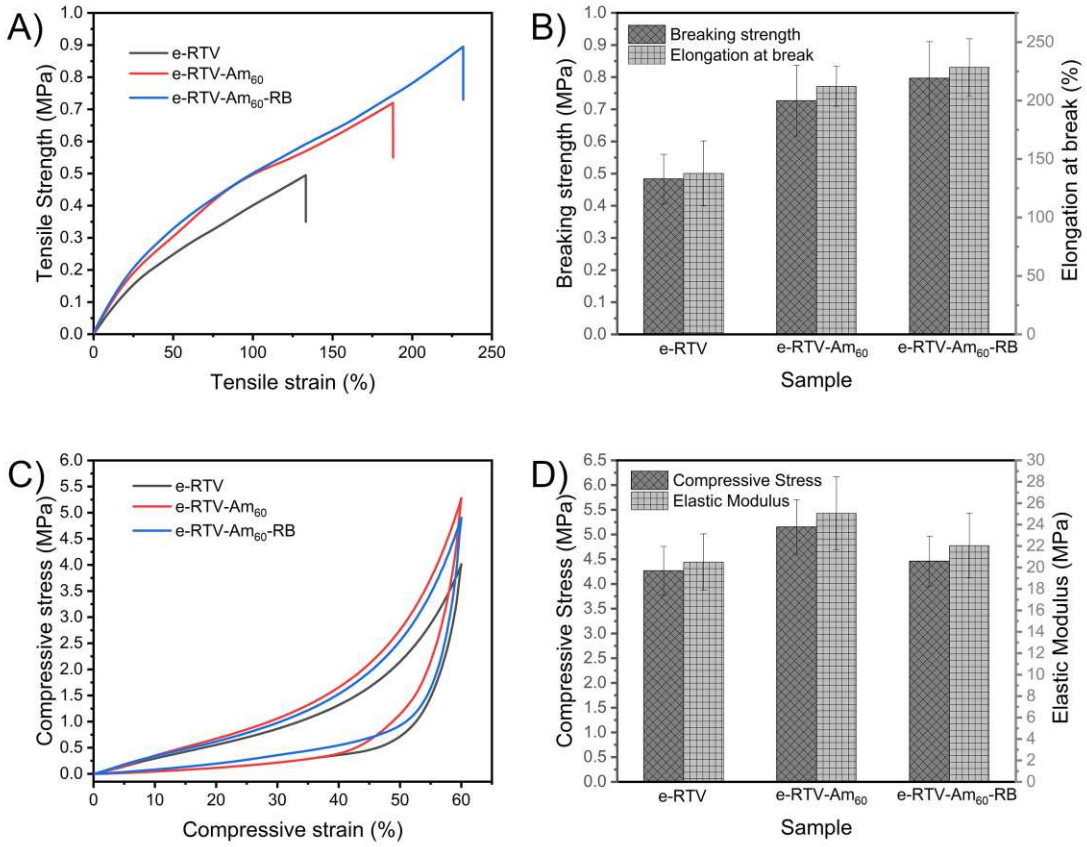


Fig. 4 The stress-strain diagram (A), breaking strength and elongation at break (%) (B), 60%

compressive stress-strain diagram (C) and compressive stress and elastic modulus (D) of e-RTV, e-RTV-Am60 and e-RTV-Am60-RB samples.

E. coli (Gram-negative) and *S. aureus* (Gram-positive) were used as the model bacteria to test the antibacterial properties of the prepared silicone rubber. From Fig. 5A, a large amount of *E. coli* was observed to be adhered to the RTV surface. However, after introducing of the Am-HQAS, the adhered *E. coli* decreased significantly. With increasing in quaternizations degree, the number of *E. coli* attached to the surface showed a decreased trend. We also examined the supernatant at various times to evaluate the growth of *E. coli* and *S. aureus* without disturbing the precipitate at the bottom of each sample containing different Am-HQAS. At regular intervals (2 to 24 hours) we determined the bacterial growth by measuring the absorbance of cultures at 600 nm. From Fig. 5C, the OD of the RTV towards *E. coli* increased significantly with the incubation time of 12 hours. In contrast, a slow linear increase for the RTV-Am_x samples was observed at the same time interval, suggesting an effective antibacterial performance. With increasing quaternization degree, the OD value of the RTV-Am_x decreased gradually in order from RTV-Am_{30} to RTV-Am_{70}. With prolonged immersing time, the OD almost unchanged. As shown in Fig. 5E, the killing rate of RTV-Am_{30}, RTV-Am_{40}, RTV-Am_{50}, RTV-Am_{60} and RTV-Am_{70} towards *E. coli* was 94.7%, 96.1%, 97.3%, 97.8% and 98.9%, respectively, which further confirmed the antibacterial activity of silicone rubber increased with increasing quaternization degree. The excellent antibacterial performance was attributed to a combined action of QAS and the long alkyl group, the hydrophobic alkyl facilitating the QAS penetrating the cell membrane and killed the bacteria. A similar trend was observed towards *S. aureus*. Compared with that of *E. coli,* these antibacterial silicone rubber showed

even better bactericidal effect towards *S. aureus* (Fig. 5B, 5D and 5F). [39]

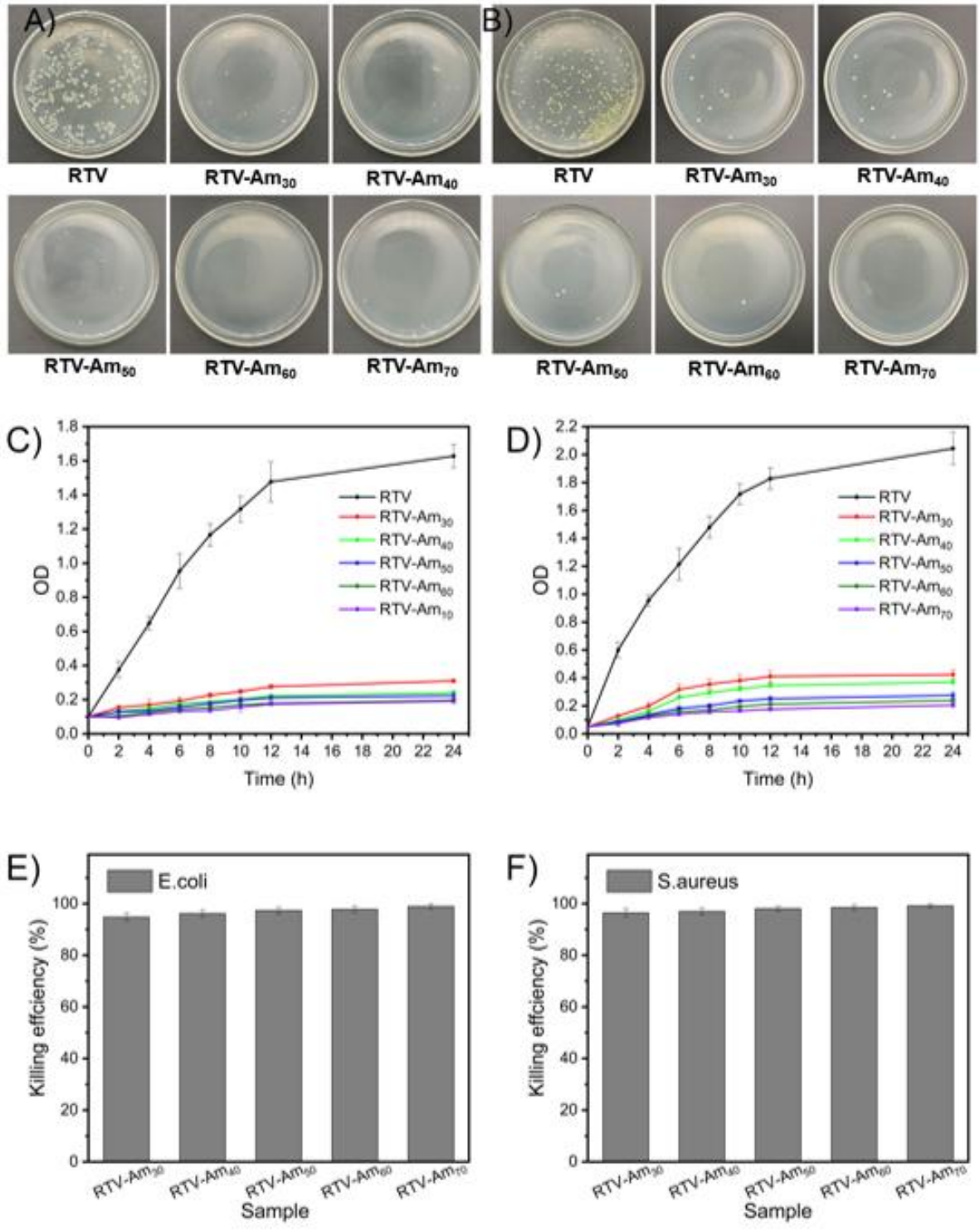


Fig. 5 The images of the E. coli (A) and S. aureus (B) adhered on the RTV and RTV-Amx samples; Bacterial growth curve of E. coli (C) and S. aureus (D) on the RTV and RTV-Amx samples; The killing efficiency of the silicone rubber towards E. coli (E) and S. aureus (F).

Considering the balance between mechanical properties and quaternary ammonium salt antibacterial properties, RTV-Am_{60} was selected to investigate the encapsulation for photosensitizer RB and photodynamic bactericidal performance. According to the encapsulation curve, the encapsulation for RB of Am_{60}-HQAS towards RB was 0.2 g/g. The release behavior of singlet oxygen $^1O_2$ produced by e-RTV-Am_{60}-RB under LED light irradiation at regular intervals was studied. From Fig. S10A, the intensity of characteristic peak at 410 nm of the capture agent DPBF decreased with increasing irradiation time from 0 to 30 min suggested singlet oxygen $^1O_2$ produced by e-RTV-Am_{60}-RB under light irradiation conditions. In the first 5 mins of LED light irradiation, the e-RTV-Am_{60}-RB sample released singlet oxygen $^1O_2$ very quickly (Fig. S10B). The release rate became slow with prolonged irradiation time. No singlet oxygen $^1O_2$ was detected after 30-min irradiation time. Based on these results, the e-RTV-Am_{60}-RB was irradiated with LED light for 30 min to produce enough singlet oxygen $^1O_2$ for further photodynamic antibacterial experiments.

From Fig. 6A, compared with the control e-RTV, e-RTV-Am_{60} showed effective antibacterial performance towards *E. coli.* The e-RTV-Am_{60}-RB showed a similar antibacterial effect. After 30-min light irradiation with LED, the OD value of e-RTV-Am_{60}-RB first increased linearly with the immersing time and finally reached saturation state (Fig. 6B). For example, the OD value of the sample, e-RTV-Am_{60}-RB-light, irradiated with 30-min light towards *E. coli* was ~0.2, a half of that of e-RTV-Am_{60}-RB, indicating exceedingly good antibacterial activity. The photodynamic antibacterial process could be repeatedly carried out many cycles without obvious changes. In addition, the killing rate of the e-RTV-Am_{60} and e-RTV-Am_{60}-RB was 94% and 95%, respectively. After light irradiation, the killing rate of the e-RTV-Am_{60}-RB-light

sample increased to 98% indicating further improved antibacterial performance (Fig. 6C).

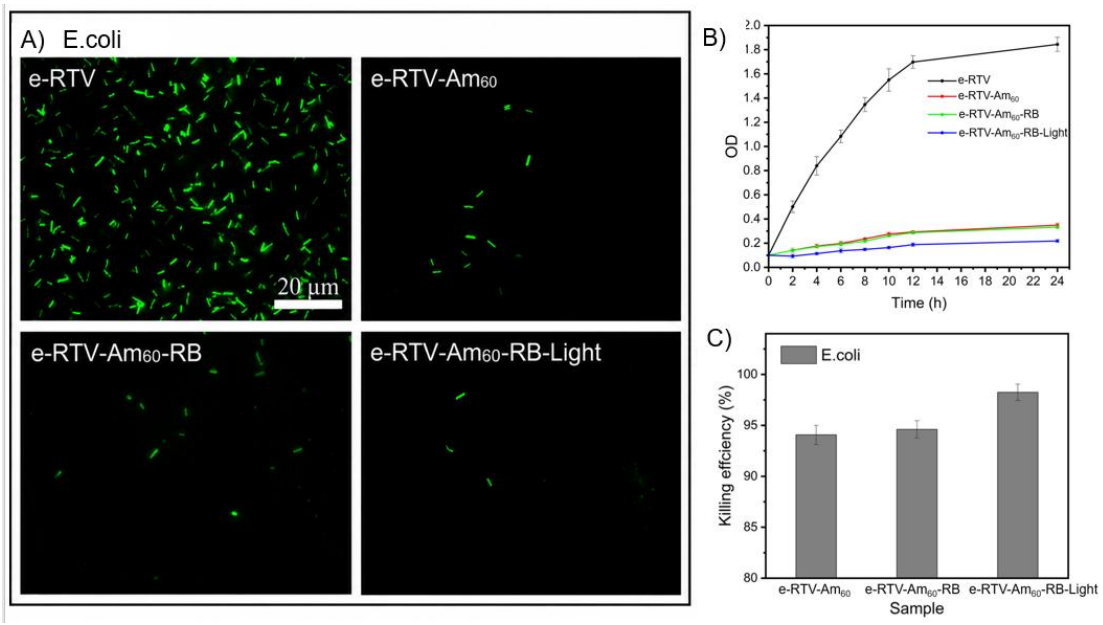


Fig. 6 (A) Confocal images of E. coli adhered on the e-RTV, e-RTV-Am60, e-RTV-Am60-RB and e-RTV-Am60-RB-Light samples; (B) Bacterial growth curve of E. coli on the various samples before and after LED light irradiation; (C) The killing efficiency of the various samples towards E. coli before and after LED light irradiation.

The samples showed a similar antibacterial activity towards *S. aureus*. Moreover, the antibacterial activity towards *S. aureus* was a little better than that of *E. coli* (Fig. S11A-C). From Fig. S12 and Fig. 7B, the density of the *S. aureus* on the e-RTV-Am$_{60}$ and e-RTV-Am$_{60}$-RB was 14×10^4 and 8×10^4 cfu/cm^2, respectively. After 30-min light irradiation, the density of the attached *S. aureus* on the sample continued to decrease. After 72 hours, the density of the *S. aureus* attached on the e-RTV-Am$_{60}$ and e-RTV-Am$_{60}$-RB was 26×10^4 and 24×10^4 cfu/cm^2, respectively. however, the density of that on e-RTV-Am$_{60}$-RB after light irradiation was only 9×10^4 cfu/cm^2, much lower than that of other samples, suggesting excellent antibacterial property. The excellent antibacterial property was attributed to a combined action of QAS functionalities and PACT progress. [40]

The adhered bacteria would weaken and even make the outer surface lose its antibacterial property due to shielding effect between the bacteria and the bactericidal coatings. In this work, the pH-sensitive cleavable betaine ester-linked bonds [41] could be hydrolyzed and resulted in a renewable bactericidal surface (Fig. 7A) facilitating to remove the adhered bacteria from the surface. As shown in Fig. 7B, a large amount of dead *S. aureus* adhered to the original sample after 72 h. After being immersed in a weak alkaline PBS buffer (pH = 8.5) for 24 hours, the attached bacteria decreased significantly. The desorption rate of e-RTV-Am_{60}, e-RTV-Am_{60}-RB and e-RTV-Am_{60}-RB-Light towards *S. aureus* was 50.1%, 54.6% and 57.7%, respectively (Fig. 7C). The desorption rate was only moderate. The possible reason is that the surface is composed of Am-HQAS and silicone rubber matrix, which results in the desorption triggered by the loss of long carbon chains in Am-HQAS only playing a partial role.

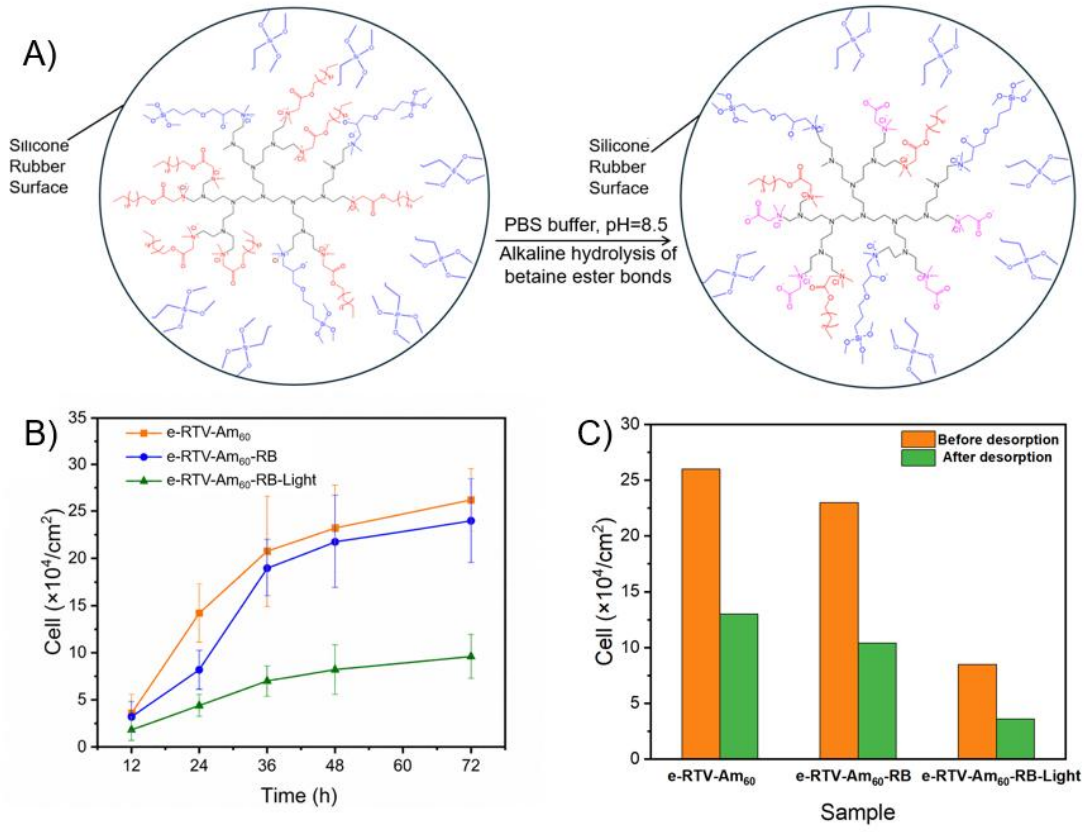


Fig. 7 (A) Alkaline hydrolysis of betaine ester bonds on the silicone rubber surface at

pH=8.5; (B) The number of S. aureus on the various silicone rubber samples at regular time interval; (C) The number of adhered S. aureus before and after desorption.

CONCLUSION

Am-HQAS nanocapsules with multiple hydrophilic QAS in the core and multiple hydrophobic long carbon chains through cleavable ester-linked bonds were first synthesized. These nanocapsules were used to encapsulate the photosensitizer RB through host-guest encapsulation. A series of antibacterial silicone rubbers containing nanocapsules with/without RB degree were developed. The contact angle of the antibacterial silicone rubber increased from 114.6° to 128.9° with increasing quaternization degree. The silicone rubber with nanocapsules showed poorer mechanical strength than the raw silicone rubber. Hydrophobic fumed silica as reinforcing agents and TEOS as co-curing agent to improve the mechanical strength of the silicone rubber. The e-RTV-Am_{60} sample exhibited a yield strength of 0.73 MPa and a compressive modulus of 25 MPa and displayed good elasticity and shape recovery ability. For *E. coli* and *S. aureus*, the silicone rubber with amphiphilic QAS nanocapsules displayed high antibacterial activity. The antibacterial activity of the silicone rubber increased with increasing quaternizations degree. The killing efficacy of e-RTV-Am_{60} reached 94% and 96% for *E. coli* and *S. aureus*, respectively. The encapsulation capacity of Am_{60}-HQAS for photosensitizer RB was 0.2 g/g. The e-RTV-Am_{60}-RB sample released singlet oxygen $^1O_2$ under LED light irradiation. After 30-min light irradiation, the killing rate of the sample increased to 98% and 99% for *E. coli* and *S. aureus*, respectively. The excellent antibacterial activity of these silicone rubber samples was attributed to a combined action of contact-killing and photodynamic process.

ASSOCIATED CONTENT

Supporting information. The Feeding ratios of the amphiphilic hyperbranched QAS nanocapsules (Table S1); The Feeding ratios of the various silicone rubber (Table S2); A standard work curve of Rose Bengal (RB) in the ultrapure water (λ=540nm) (Fig. S1); A plot of the encapsulating capability *vs* the RB concentration (Fig. S2); ^{1}H-NMR spectra of Am_x-HQAS (Fig. S3); The static water contact angle (A) and the contact angle images (B)of RTV and RTV-AM_x (Fig. S4); The static water contact angle (A) and the contact angle images (B) of e-RTV, e-RTV-AM_{60} and e-RTV-AM_{60}-RB (Fig. S5); The stress-strain diagram of the various silicone rubber samples (Fig. S6); 60% compressive stress-strain diagram of the various silicone rubber samples (Fig. S7); The compressive stress-strain diagram of the various silicone rubber samples during the 10 loading-unloading cycles with 60% deformation (A: RTV, B: RTV-AM_{30}, C: RTV-AM_{40}, D: RTV-AM_{50}, E: RTV-AM_{60}, F: RTV-AM_{70}) (Fig. S8); The compressive stress-strain diagram of the various silicone rubber samples during the 10 loading-unloading cycles with 60% deformation (A: e-RTV, B: e-RTV-AM_{60}, C: e-RTV-AM_{60}-RB) (Fig. S9); UV scanning spectrum of DPBF of e-RTV-AM60-RB under LED light irradiation; changing trend of intensity of characteristic absorption peak (410 nm) of DPBF of e-RTV-AM60-RB under LED light irradiation (Fig. S10); Confocal images of *S. aureus* adhered on the e-RTV, e-RTV-Am_{60} , e-RTV-Am_{60}-RB and e-RTV-Am_{60}-RB-Light samples; Bacterial growth curve of *S. aureus* on the various silicone rubber before and after LED light irradiation; The killing efficiency of the various silicone rubbers towards *S. aureus* before and after LED light irradiation (Fig. S11); Fluorescence image of the e-RTV-Am_{60} , e-RTV-Am_{60}-RB and e-RTV-Am_{60}-RB-Light samples after culturing in *S. aureus* at regular time interval

(Fig. S12)

STATEMENTS AND DECLARATIONS

Funding
This research was supported by Zhejiang Provincial Natural Science Foundation (LTGY23E030004), company projects (KYY-HX-20241099, KYY-HX-20220654, and KYY-HX-20200193) and Xianju County Science and Technology Bureau commissioned service project (KYY-HX-20240829).

Competing Interests
The authors declare that they have no competing interests.

Data Availability
The data that support the findings of this study are available from the corresponding author upon reasonable request.

REFERENCES

1. Wang, G.; Li, A.; Zhao, W.; Xu, Z.; Ma, Y.; Zhang, F.; Zhang, Y.; Zhou, J.; He, Q., A Review on Fabrication Methods and Research Progress of Superhydrophobic Silicone Rubber Materials. *Adv Mater Interfaces* 2021, *8* (1), 2001460.
2. Shit, S. C.; Shah, P., A Review on Silicone Rubber. *National Academy Science Letters* 2013, *36* (4), 355-365.
3. Gao, S.; Liu, Z.; Zeng, W.; Zhang, Y.; Zhang, F.; Wu, D.; Wang, Y., Biocompatible Hydrogel Coating on Silicone Rubber with Improved Antifouling and Durable Lubricious Properties. Gels 2024, 10 (10), 647.
4. Gao, S.; Zeng, W.; Liu, Z.; Zhang, F.; Zhang, Y.; Liu, X.; Wu, D.; Wang, Y., Dual-Function Hydrogel Coating on Silicone Urinary Catheters with Durable Antibacterial Property and Lubricity. Gels 2025, 11 (2), 128.
5. Lawrence, E. L.; Turner, I. G., Materials for urinary catheters: a review of their history and development in the UK. *Med Eng Phys* 2005, *27* (6), 443-453.
6. Chen, P.-H.; Chen, G.-H.; Tsai, W.-B., Innovative Polymeric Coatings with Dual Antifouling and Light-Activated Bactericidal Functions for Urinary Catheter Applications. Polymers 2024, 16 (21), 2974.
7. Garvey, M., Medical Device-Associated Healthcare Infections: Sterilization and the Potential of Novel Biological Approaches to Ensure Patient Safety. International Journal of Molecular Sciences 2023, 25 (1), 201.
8. VanEpps, J. S.; Younger, J. G., Implantable Device-Related Infection. *Shock* 2016, *46* (6).
9. Parada, G.; Yu, Y.; Riley, W.; Lojovich, S.; Tshikudi, D.; Ling, Q.; Zhang, Y.; Wang, J.; Ling, L.; Yang, Y.; Nadkarni, S.; Nabzdyk, C.; Zhao, X., Ultrathin and Robust Hydrogel Coatings on Cardiovascular Medical Devices to Mitigate Thromboembolic and Infectious Complications. *Adv Healthc Mater* 2020, *9* (20), 2001116.
10. Timsit, J.-F.; Dubois, Y.; Minet, C.; Bonadona, A.; Lugosi, M.; Ara-Somohano, C.; Hamidfar-Roy, R.; Schwebel, C., New materials and devices for preventing catheter-related infections. *Ann Intensive Care* 2011, *1* (1), 34.
11. Tischer, M.; Pradel, G.; Ohlsen, K.; Holzgrabe, U., Quaternary Ammonium Salts and Their

Antimicrobial Potential: Targets or Nonspecific Interactions? *Chemmedchem* 2012, *7* (1), 22-31.

12. Dong, F.; Jia, T.; Wang, Q.; Liu, Y.; Ma, L.; Li, S.; Tang, X.; Feng, S., Preparation of intrinsic antibacterial silicone rubber with matrix tethering quaternary ammonium salt groups. *Materials Today Communications* 2021, *26*, 101695.

13. Pan, Z.; Liu, Z.; Yang, S.; Shen, Z.; Wu, Y.; Liu, Y.; Li, J. F.; Wang, L., Covalent Grafting of Quaternary Ammonium Salt-Containing Polyurethane onto Silicone Substrates to Enhance Bacterial Contact-Killing Ability. Polymers 2024, 17 (1), 17.

14. Gottenbos, B.; van der Mei, H. C.; Klatter, F.; Nieuwenhuis, P.; Busscher, H. J., In vitro and in vivo antimicrobial activity of covalently coupled quaternary ammonium silane coatings on silicone rubber. *Biomaterials* 2002, *23* (6), 1417-1423.

15. Asri, L. A. T. W.; Crismaru, M.; Roest, S.; Chen, Y.; Ivashenko, O.; Rudolf, P.; Tiller, J. C.; van der Mei, H. C.; Loontjens, T. J. A.; Busscher, H. J., A Shape-Adaptive, Antibacterial-Coating of Immobilized Quaternary-Ammonium Compounds Tethered on Hyperbranched Polyurea and its Mechanism of Action. *Adv Funct Mater* 2014, *24* (3), 346-355.

16. Zhang, J.; Tan, W.; Li, Q.; Liu, X.; Guo, Z., Preparation of cross-linked chitosan quaternary ammonium salt hydrogel films loading drug of gentamicin sulfate for antibacterial wound dressing. *Mar Drugs* 2021, *19* (9), 479.

17. Zhao, C.; Zhou, L.; Chiao, M.; Yang, W., Antibacterial hydrogel coating: Strategies in surface chemistry. *Adv Colloid Interfac* 2020, *285*, 102280.

18. Wei, S.; Liu, X.; Zhou, J.; Zhang, J.; Dong, A.; Huang, P.; Wang, W.; Deng, L., Dual-crosslinked nanocomposite hydrogels based on quaternized chitosan and clindamycin-loaded hyperbranched nanoparticles for potential antibacterial applications. *Int J Biol Macromol* 2020.

19. Li, M. X.; Rong, M. Z.; Zhang, M. Q., Enhancement of mechanochemical self-blocking and self-healing of early minor damages in polymers through hyperbranched architecture. eXPRESS Polymer Letters 2021, 15 (8), 781-790.

20. Santoro, O.; Izzo, L., Antimicrobial Polymer Surfaces Containing Quaternary Ammonium Centers (QACs): Synthesis and Mechanism of Action. International Journal of Molecular Sciences 2024, 25 (14), 7587.

21. Lainioti, G.C.; Druvari, D., Designing Antibacterial-Based Quaternary Ammonium Coatings (Surfaces) or Films for Biomedical Applications: Recent Advances. International Journal of Molecular Sciences 2024, 25 (22), 12264.

22. Xiao, Q.; Mai, B.; Nie, Y.; Yuan, C.; Xiang, M.; Shi, Z.; Wu, J.; Leung, W.; Xu, C.; Yao, S. Q.; Wang, P.; Gao, L., Correction to "In Vitro and In Vivo Demonstration of Ultraefficient and Broad-Spectrum Antibacterial Agents for Photodynamic Antibacterial Chemotherapy". *Acs Appl Mater Inter* 2022, *14* (39), 45076-45076.

23. Hu, X.; Zhang, H.; Wang, Y.; Shiu, B.-C.; Lin, J.-H.; Zhang, S.; Lou, C.-W.; Li, T.-T., Synergistic antibacterial strategy based on photodynamic therapy: Progress and perspectives. *Chem Eng J* 2022, *450*, 138129.

24. Anas, A.; Sobhanan, J.; Sulfiya, K. M.; Jasmin, C.; Sreelakshmi, P. K.; Biju, V., Advances in photodynamic antimicrobial chemotherapy. *Journal of Photochemistry and Photobiology C: Photochemistry Reviews* 2021, *49*, 100452.

25. Fischer, T.; Suttor, S.; Mansi, S.; Osthues, L.; Mela, P., Antimicrobial silicone rubbers based on photocatalytically active additives. *J Appl Polym Sci* 2021.

26. Wainwright, M., Photodynamic antimicrobial chemotherapy (PACT). *The Journal of antimicrobial*

chemotherapy 1998, *42* (1), 13-28.
27. Li, M.; Mai, B.; Wang, A.; Gao, Y.; Wang, X.; Liu, X.; Song, S.; Liu, Q.; Wei, S.; Wang, P., Correction: Photodynamic antimicrobial chemotherapy with cationic phthalocyanines against Escherichia coli planktonic and biofilm cultures. *Rsc Adv* 2022.
28. Dube, E., Antimicrobial Photodynamic Therapy: Self-Disinfecting Surfaces for Controlling Microbial Infections. Microorganisms 2024, 12 (8), 1573.
29. Cantelli, A.; Piro, F.; Pecchini, P.; Di Giosia, M.; Danielli, A.; Calvaresi, M., Concanavalin A-Rose Bengal bioconjugate for targeted Gram-negative antimicrobial photodynamic therapy. *Journal of Photochemistry and Photobiology B: Biology* 2020, *206*, 111852.
30. Gu, J.; An, Q.; Huang, M.-C.; Ge, P.; Xue, C.-H., Self-Cleaning Antibacterial Composite Coating of Fluorinated Acrylic Resin and Ag/SiO2 Nanoparticles with Quaternary Ammonium. Polymers 2024, 16 (13), 1885.
31. Sharma, S. K.; Dai, T.; Kharkwal, G. B.; Huang, Y.-Y.; Huang, L.; De Arce, V. J. B.; Tegos, G. P.; Hamblin, M. R., Drug discovery of antimicrobial photosensitizers using animal models. *Curr Pharm Design* 2011.
32. Li, P.; Yin, R.; Cheng, J., Bacterial Biofilm Formation on Biomaterials and Approaches to Its Treatment and Prevention. International Journal of Molecular Sciences 2023, 24 (14), 11680.
33. Wang, N.; Wang, X.; Lang, J.; Hu, Z.; Zhang, H., Synthesis and Characterization of Hyperbranched and Organosilicone Modified Waterborne Polyurethane Acrylates Photosensitive Resin. Polymers 2021, 13 (13), 2039.
34. Han, J.; Zheng, Y.; Zheng, S.; Li, S.; Hu, T.; Tang, A.; Gao, C., Water soluble octa-functionalized POSS: all-click chemistry synthesis and efficient host-guest encapsulation. *Chem Commun* 2014.
35. Han, J.; Chen, Q.; Shen, Y.; Liu, Z.; Hao, X.; Zhong, M.; Zhao, Z.; Bockstaller, M. R., Click-Chemistry Approach toward Antibacterial and Degradable Hybrid Hydrogels Based on Octa-Betaine Ester Polyhedral Oligomeric Silsesquioxane. *Biomacromolecules* 2020, *21* (9), 3512-3522.
36. Nsubuga, A.; Mandl, G. A.; Capobianco, J. A., Investigating the reactive oxygen species production of Rose Bengal and Merocyanine 540-loaded radioluminescent nanoparticles. *Nanoscale Advances* 2021.
37. Entradas, T.; Waldron, S.; Volk, M., The detection sensitivity of commonly used singlet oxygen probes in aqueous environments. *Journal of Photochemistry and Photobiology B: Biology* 2020.
38. Weiss, E.; Berl, A.; Shir-az, O.; Bilal, B. S.; Weiss, E. I.; Paitan, Y.; Zaltsman, N.; Golberg, A.; Shalom, A., Quaternary Ammonium Silica Nanoparticles for Antimicrobial Implantable Medical Devices: An In Vitro Study. Life 2024, 14 (12), 1654.
39. Navarrete-Germán, L.; Gómez-Lázaro, B.; López-Saucedo, F.; Bucio, E., Antimicrobial Functionalization of Silicone-graft-poly(N-vinylimidazole) Catheters. Molecules 2024, 29 (10), 2225.
40. Cheng, C.-H.; Zeng, X.-Z.; Chiu, W.-Y.; Lin, J.-C., A Facile Surface Modification Scheme for Medical-Grade Titanium and Polypropylene Using a Novel Mussel-Inspired Biomimetic Polymer with Cationic Quaternary Ammonium Functionalities for Antibacterial Application. Polymers 2024, 16 (4), 503.
41. Han, J.; Chen, Q.; Feng, Y.; Shen, Y.; Wu, D.; Zhong, M.; Zhang, Q.; Zhao, Z.; Zhai, Y.; Bockstaller, M. R. Seawater-Degradable and Antibacterial Epoxy Thermosets Employing Betaine Ester Linkages. ACS Appl. Polym. Mater. 2023, 5 (5), 3298-3305.

For Table of Contents Use Only

Host-guest Encapsulation of Photosensitizer to Construct Antibacterial Silicone Rubber: Enhanced Homogeneity and Dual-action.

Jin Han[1], Yaocheng Zhu[1], Ziqiang Zhang[1], Taolei Qiu[1], Lei Wang[1], Zhengping Zhao[1], Xiaoxue Yin[2], Dawei Zhang[2], Kun Shen[2,*], Dong Xu[3], Boshi Yu[3], Tongdong Shen[4], Zhixiong Liu[5]

Supplementary Files

This is a list of supplementary files associated with this preprint. Click to download.

- Supportinginformation.docx